

# Complexity reduction in self-interaction-free density functional calculations using the Fermi-Löwdin self-interaction correction method

Selim Romero,<sup>1</sup> Yoh Yamamoto,<sup>2</sup> Tunna Baruah,<sup>1,2</sup> and Rajendra R. Zope<sup>1,2</sup>

<sup>1</sup>Computational Science Program, The University of Texas at El Paso, El Paso, Texas 79968

<sup>2</sup>Department of Physics, University of Texas at El Paso, TX, 79968

(Dated: 10 August 2023)

Fermi-Löwdin (FLO) self-interaction-correction (SIC) (FLOSIC) method uses symmetric orthogonalized Fermi orbitals as localized orbitals in one-electron SIC schemes resulting in a formal reduction in the scaling of SIC methods (e.g. Perdew-Zunger SIC (PZSIC) method) but requires a set of Fermi orbital descriptors used to define the FLOs which can be computationally taxing. Here, we propose to simplify the SIC calculations using a selective orbital scaling self-interaction correction (SOSIC) by removing SIE from a select set of orbitals that are of interest. We illustrate the approach by choosing a valence set of orbitals as active orbitals in the SOSIC approach. The results obtained using the vSOSIC scheme are compared with those obtained with PZSIC which corrects for SIE of all orbitals. The comparison is made for atomization energies, barrier heights, ionization energies (absolute highest occupied orbital [HOO] eigenvalues), exchange coupling constant and spin densities of Cu-containing complexes, and vertical detachment energies (VDE) of water cluster anions. The agreement between the two methods is within a few percent for the majority of the properties. The MAE in the VDE (absolute HOO eigenvalue) of water cluster anions with vSOSIC-PBE with respect to benchmark CCSD(T) results is only 15 meV making vSOSIC-PBE an excellent alternative to the CCSD(T) to obtain the VDE of water cluster anions. The vSOSIC calculation on  $[\text{Cu}_2\text{Cl}_6]^{2-}$  complex demonstrates that, in addition to the cost savings from using fewer orbitals to account for SIC, the FOD optimization in vSOSIC is also substantially smoother and faster.

## INTRODUCTION

The low computational expense combined with relatively good accuracy of density functional theory (DFT)<sup>1,2</sup> has made it a quantum mechanical method of choice to study the electronic structure of various types of materials, from atoms and molecules to nanostructures to periodic materials. Practical DFT calculations require approximation to the unknown exchange-correlation functional, and numerous density functional approximations (DFAs) with varying degrees of complexity have been proposed. Many failures of the DFAs have been ascribed to the self-interaction error (SIE) present in the approximate exchange-correlation functionals. The problem arises since the self-Coulomb energy is not completely canceled by the self-exchange energy when the exact, but unknown, exchange-correlation functional is approximated. A few illustrative examples of the failures of DFA are charge delocalization in proteins<sup>3</sup>, completely different charge distribution on Kevan structure for the solvated electron,<sup>4</sup> spurious charge transfer in organic acid-base co-crystals<sup>5</sup>, severe overestimation of hyperpolarizabilities in conjugated molecules,<sup>6</sup> structural distortion in the electron polaron model systems,<sup>7</sup> a lack of size-intensivity of ionization potential<sup>8</sup> and so on. The self-interaction correction (SIC) methods to remove SIE in an orbital-wise manner were devised long ago.<sup>9-17</sup>

The most well-known one-electron SIC method is the Perdew-Zunger SIC (PZSIC)<sup>11,14</sup> method wherein an orbital by orbital correction is applied to the DFA total energy<sup>11</sup>. The PZSIC energy is

given by

$$E^{PZSIC}[\rho_{\uparrow}, \rho_{\downarrow}] = E^{DFA}[\rho_{\uparrow}, \rho_{\downarrow}] - \sum_{i\sigma}^{occ} \{U[\rho_{i\sigma}] + E_{XC}^{DFA}[\rho_{i\sigma}, 0]\} \quad (1)$$

Here,  $E^{DFA}$  is the DFA total energy,  $\rho_{\uparrow}$ ,  $\rho_{\downarrow}$ , and  $\rho_{i\sigma}$  are up spin, down spin, and orbital densities, respectively;  $U[\rho_{i\sigma}]$  and  $E_{XC}^{DFA}[\rho_{i\sigma}, 0]$  are the Coulomb and approximate exchange energies. The PZSIC energy minimization corresponds to finding an optimal unitary transformation of canonical Kohn-Sham orbitals and results in a set of  $M(M-1)/2$  conditions (for  $M$  occupied orbitals) known as the localization equations.<sup>18,19</sup> These equations are given by

$$\langle \phi_i | V_i - V_j | \phi_j \rangle = 0. \quad (2)$$

Here,  $V_i$  is the sum of Coulomb and exchange-correlation potential of the  $i^{\text{th}}$  orbital. Although not as popular as standard gradient-based DFAs, a number of researchers have adopted PZSIC<sup>15,20-56</sup> Many implementations of the PZSIC use localized orbitals obtained using various criteria.<sup>37,57,58</sup> In 1984, Luken and Culberson observed that properties of the Fermi hole can be used to transform canonical orbitals into a set of localized orbitals.<sup>59,60</sup> As these orbitals are not orthogonal, they proposed a symmetric orthogonalization procedure to obtain a set of orthogonal orbitals. In 2014, Pederson, Ruszinsky and Perdew used these orbitals, which they called Fermi-Löwdin orbitals, to obtain PZSIC energy.<sup>61</sup> This results in a unitary invariant

implementation of the PZSIC energy functional (Eq. 1). The Fermi orbitals (FO)<sup>59,60</sup> are given by

$$F_{j\sigma}(\vec{r}) = \frac{\sum_i \psi_{i\sigma}(\vec{a}_{j\sigma}) \psi_{i\sigma}(\vec{r})}{\sqrt{\rho_{\sigma}(\vec{a}_{j\sigma})}}. \quad (3)$$

Here, the sum of  $i$  represents the sum over Kohn-Sham orbitals ( $\psi_{i\sigma}$ ) and  $j$  is the FO index (local orbital),  $\rho_{\sigma}$  is the total electron spin density, and  $\vec{a}_j$  is the so-called Fermi orbital descriptor (FOD) position. The Fermi orbitals are further orthogonalized using the Löwdin method to give the Fermi-Löwdin orbitals (FLOs). The PZSIC energy is minimized by varying the FOD positions in combination with a conjugate gradient or BFGS algorithm.<sup>62,63</sup> The FLOSIC method<sup>61-66</sup> ensures size extensivity, as well as unitary invariance of the total energy. It also simplifies the problem since instead of the satisfaction of  $N(N-1)/2$  equations only  $3N$  variables, where  $N$  is the number of orbitals, need to be optimized. This results in a significant reduction in the formal cost of the SIC calculations.

The FLOSIC method has been used to study a wide range of chemical and physical properties.<sup>11,34,36,43,67-102</sup> As mentioned above, obtaining the SIC energy in the PZSIC requires the determination of the optimal FOD positions. In practice, however, the optimization of FOD is a slow process due to the complicated/shallow potential energy surface generated by the FODs, especially for systems containing transition metal (TM) atoms. The FOD optimization of systems with TM atoms is particularly difficult and can often require a few hundred steps. Moreover, the number of steps required grows as the number of FODs increases. Our experience with the FOD optimizations shows that the difficulties primarily arise from the optimization of core FODs. To alleviate this problem, approaches such as freezing the core FOD for the 1s orbitals or the use of pseudopotential have been adopted in formance of the r2SCAN functional with PZSIC and vSOSIC methsome FLOSIC calculations on the transition metal and some organic complexes<sup>80,85,103</sup>.

In this work, we propose a simplification of the FLOSIC calculation by selecting a subset of Kohn-Sham orbitals in constructing FLOs for the SIC calculations. Since the physical properties of systems are determined mainly by the valence electrons, we choose this subset to be the valence orbitals. We validate this approach by performing extensive tests on a variety of systems on several different properties. We show that the proposed simplified scheme, which results in a substantial reduction in the number of parameters (FODs) to be optimized, reproduces results of the *full* all-electron FLOSIC method within 1-2 kcal/mol and that for many properties, in fact, provides slightly improved results. We have applied the present approach to the lowest three rungs of functionals, namely, local spin density approximation (LSDA), Perdew-Burke-Ernzerhof (PBE) generalized gradient approximation (GGA), and r<sup>2</sup>SCAN meta-GGA functionals. Though not the primary focus of

this work, we also report the assessment of the SIC-r<sup>2</sup>SCAN approach. We believe this is the first time SIC-r<sup>2</sup>SCAN approach has been assessed for a range of electronic properties. We also demonstrate that accurate estimates of the vertical detachment energies of water cluster anions can be obtained using the simplest version of the SOSIC, in which only the orbital containing the extra electron in the water cluster anions is corrected for the SIE.

The details about the present approach and its implementation are provided in the next section followed by results and discussion.

## II. METHODOLOGY

We divide the  $N$  occupied Kohn-Sham (KS) orbitals into groups of  $P$  passive and  $(N-P)$  active orbitals such that the corrected exchange-correlation energy can be written as<sup>75</sup>

$$E_{XC}^{SOSIC-DFA} = E_{XC}^{DFA}[\rho_{\uparrow}, \rho_{\downarrow}] - \sum_{i\sigma=1}^P X_{i\sigma}^k (U[\rho_{i\sigma}] + E_{XC}^{DFA}[\rho_{i\sigma}, 0]) - \sum_{i\sigma=P+1}^{occ} Y_{i\sigma}^k (U[\rho_{i\sigma}] + E_{XC}^{DFA}[\rho_{i\sigma}, 0]). \quad (4)$$

Here,  $X_{i\sigma}^k$  and  $Y_{i\sigma}^k$  can be considered as scaling factors that can be determined using various criteria.<sup>67,75</sup> The value of  $P$  should be chosen carefully. For example, by applying full SIC correction to the orbitals that participate in the stretched bonds and scaling down SIC for other orbitals, Yamamoto and coworkers were able to obtain barrier heights of BH6 dataset within the chemical accuracy<sup>75</sup> using this selective orbital scaling SIC (SOSIC). As our purpose in this work is to simplify the SIC approach to improve its computational efficiency, we choose  $P$  to be the core orbitals with the factors  $X_{i\sigma}^k = 0$  and  $Y_{i\sigma}^k = 1$ . This amounts to removing the SIE only from the valence electrons. This method of selectively applying SIC to the valence electron will be referred to as vSOSIC hereafter.

We choose the  $P$  core electrons as shown in Table I. For example, in the case of manganese which has an electronic configuration  $[\text{Ar}]4s^23d^5$ ,  $P$  is 10, i.e., only the electrons in the  $3s, 3p, 3d$  and  $4s$  are considered for the SIC calculations. Previous calculations indicate that a full shell should be included to allow shell hybridization in the SIC calculations. It is noted that the FOD positions for atoms often follow the shell structure such that four FODs transcribe to the second shell ( $2s, 2p$ ), 9 for the third shell ( $3s, 3p, 3d$ ), etc. Therefore, the use of  $[\text{Ar}]$  core, in this case, is not recommended. The 3d transition metal atoms from scandium to zinc are assigned a neon core similar to a small core in the effective core potential (SC ECP) schemes. Such a choice considerably simplifies SIC calculations due to a reduction in the time-consuming task of calculating orbital-

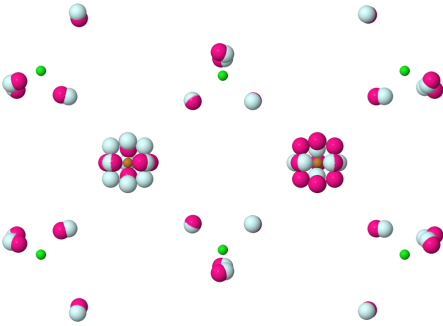


FIG. 1:  $[\text{Cu}_2\text{Cl}_6]^{2-}$  SOSIC Fermi orbital descriptors. The magenta (grey) FOD corresponds spin-up (down) channel. The orange (green) dots represent copper (chlorine) atom positions. Instead of 162 FODs, vSOSIC uses only 82 FODs.

wise SIC potentials. More importantly, it also facilitates the optimization of the FODs since often FODs in all orbital FLOSIC calculations are more difficult to optimize. We note in passing that the proposed scheme also permits the application of SIC in selected regions in space in the spirit of embedding approaches for applications such as single-atom catalysis. Such applications will be pursued in subsequent studies.

In the vSOSIC method, localized Fermi orbitals are constructed from the valence Kohn-Sham orbitals and valence electron density as,

$$F_{j\sigma}(\vec{r}) = \frac{\sum_{i=P+1}^N \psi_{i\sigma}(\vec{a}_{j\sigma}) \psi_{i\sigma}(\vec{r})}{\sqrt{\rho_{\sigma}^{\text{val}}(\vec{a}_{j\sigma})}}. \quad (5)$$

Here,  $\rho_{\sigma}^{\text{val}}(\vec{a}_{j\sigma}) = \sum_{i=P+1}^N |\psi_{i\sigma}(\vec{a}_{j\sigma})|^2$ ,  $N$  is the number of electrons and  $\vec{a}_{j\sigma}$  are the Fermi-orbital descriptors. The Fermi-Löwdin orbitals ( $\phi_{i\sigma}(\vec{r})$ ) are obtained after symmetric orthogonalization of the Fermi orbitals from Eq. (5). These FLOs are used to compute the SIC potentials and energies. Naturally, vSOSIC requires less number of FODs than the number of occupied orbitals. FODs for  $[\text{Cu}_2\text{Cl}_6]^{2-}$  are shown in Fig. 1 as an example where 82 FODs are present instead of the 162 electrons present in the molecule.

Self-consistency can be obtained either using optimized effective potential within the Kriger-Li-Ifarate approximation<sup>65</sup> or using the Jacobi update approach.<sup>64</sup> We have used the Jacobi update approach in this work. Fig. 2 pictorially presents how the vSOSIC Hamiltonian is constructed. We first construct a SIC Hamiltonian as de-

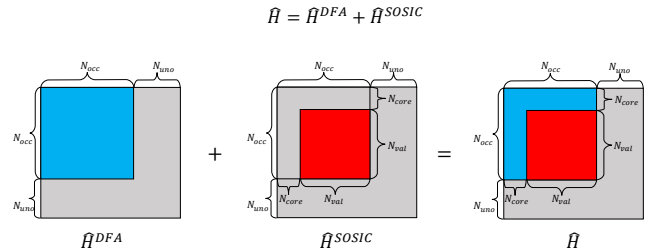


FIG. 2: Visual representation of the DFA+SIC Hamiltonian construction in the vSOSIC approach.

scribed by Yang *et al.*<sup>64</sup> as

$$H_{\sigma} = H_{\sigma}^{\text{DFA}} + \sum_{i,j=P+1}^{N_{\sigma}} \frac{1}{2} (V_{ij}^{i\sigma} + V_{ji}^{j\sigma}) |\phi_{i\sigma}\rangle \langle \phi_{j\sigma}| \quad (6)$$

where,

$$V_{ij}^{i\sigma} = \langle \phi_{i\sigma} | V^{i\sigma} | \phi_{j\sigma} \rangle$$

with  $V^{i\sigma}$  being the SIC potential for the  $i$ th orbital of spin  $\sigma$ . For the vSOSIC case, the SIC part of the Hamiltonian has  $M \times M$  non-vanishing elements where  $M = N - P$ . The Jacobi update approach is used to derive the orthogonal eigenvectors. Once the self-consistency is achieved for a given FOD configuration, the forces on the FODs are calculated<sup>62,63</sup> and the FOD positions are optimized either using the LBFGS or conjugate gradient schemes.<sup>104</sup> We show in Fig. 3 the SOSIC algorithm with Jacobi approach.

The vSOSIC calculations are performed for the *non-empirical* functionals at the three lowest rungs of functional ladder. These are LSDA, GGA, and meta-GGA. We choose PW92 correlation functional<sup>105</sup> for the LSDA, PBE parameterization for the GGA,<sup>106,107</sup> and r<sup>2</sup>SCAN meta-GGA functionals.<sup>108</sup> For comparison, we have also included PZSIC calculations using FLOs where FLOs are constructed using all Kohn-Sham orbitals as in previous FLOSIC calculations. The PZSIC-LSDA and PZSIC-PBE calculations have been reported earlier while the PZSIC-r<sup>2</sup>SCAN results reported herein are new results.

We have modified the FLOSIC code<sup>109</sup> for the work described here. The NRLMOL basis set is used for all calculations in this work.<sup>110</sup> For the vertical detachment energy calculations of water cluster anions, we used the NRLMOL basis set<sup>110</sup> with extra diffused functions to account for the anionic nature of the water clusters.<sup>111</sup> The Gaussian exponents for the extra functions are provided by Yagi *et al.*<sup>112</sup> where their values are  $9.87 \times 10^{-3}$ ,

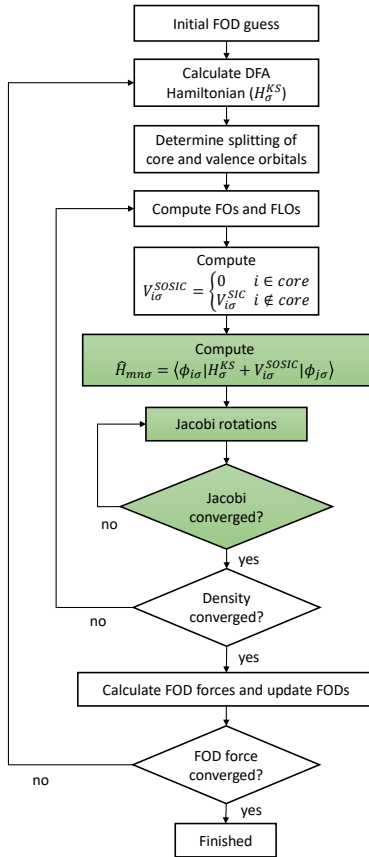


FIG. 3: vSOSIC algorithm flowchart for Jacobi rotations approach.

$8.57 \times 10^{-3}$ , and  $3.72 \times 10^{-3}$  for oxygen s and p, and hydrogen s functions, respectively.

As mentioned earlier this is the first work that reports FLOSIC-r<sup>2</sup>SCAN calculations on a wider range of properties. We therefore briefly comment on the numerical details of SIC calculations with r<sup>2</sup>SCAN. In our earlier works,<sup>74,88</sup> we have implemented and discussed the performance and numerical sensitivity of the SCAN and rSCAN functionals. The sensitivity of the SCAN functional to the choice of the numerical grid has been noted in a few studies.<sup>74,88,113–116</sup> The numerical instability of SCAN is primarily due to its interpolation function, which is smoothed out in rSCAN and r<sup>2</sup>SCAN functionals. The r<sup>2</sup>SCAN functional<sup>108</sup> is numerically more stable than the original SCAN and requires a less dense grid. We note that SIC calculations typically require denser numerical

TABLE I: Sets of criteria for determining the value  $P$  in Eq. (4) for hydrogen up to the barium atom in order to differentiate core and valence electrons.

Z	Criteria #1 Large core (LC)		Criteria #2 Small core (SC)	
	No. core	core-shell	No. core	core-shell
1-4	0		0	
5-12	2	He: $1s^2$	2	He: $1s^2$
13-30	10	Ne: [He] $2s^2 2p^6$	10	Ne: [He] $2s^2 2p^6$
31-48	28	[Ar] $3d^{10}$	10	Ne: [He] $2s^2 2p^6$
49-56	46	[Kr] $4d^{10}$	28	[Ar] $3d^{10}$

<sup>a</sup> Reference 117

grids than the standard DFA calculations as the SIC contributions to the Hamiltonian/Fock matrix elements and SIC energy corrections are evaluated using the orbital densities that can vary far more rapidly than the total spin densities used in evaluating corresponding DFA contributions. Our earlier work has shown that FLOSIC calculations with SCAN functional typically requires very dense grids with about 140000 grid points per atom. We have examined the numerical needs of r<sup>2</sup>SCAN in the FLOSIC calculations. The details are in the supplementary information. We find that FLOSIC-r<sup>2</sup>SCAN calculations require a factor of 2-4 times fewer grid points than FLOSIC-SCAN calculations. To describe the energy landscape in covalent bond stretching or reaction pathway, however, it requires a denser mesh than the default mesh of the FLOSIC code. The numerical mesh used in the present SIC-r<sup>2</sup>SCAN calculations has roughly 1.1–1.5 times more grid points than the mesh requirements of the SIC-LSDA.

### III. RESULTS AND DISCUSSION

In this section, we first present the results on energy-related properties such as atomization energies, reaction barrier heights, ionization potentials, and magnetic exchange coupling parameters using the present vSOSIC approach to assess its performance in comparison to the *all-orbital* PZSIC results in which all canonical KS orbitals are included in the construction of the Fermi-Löwdin orbitals and SIC energy is calculated by summing SIC energy contribution of *all* orbitals.

## A. Atomization energies

We evaluated the performance of vSOSIC atomization energies (AEs) on the AE6<sup>118</sup> dataset and a set of 37 molecules from the G2/97 dataset.<sup>119</sup> AE6 consists of the atomization energies of six molecules and is typically used as a small representative benchmark set of the larger main group atomization energy (MGAE109) dataset. We calculated atomization energies as follows,  $AE = \sum_i^{N_{atoms}} E_i - E_{mol}$ , where  $E_i$  is the energy of the atoms and  $E_{mol}$  is the energy of the molecule. The mean absolute errors (MAEs) for the AE6 set are derived by comparing against the values from Ref. 118 and are shown in Table II. Since the vSOSIC includes a smaller set of orbitals, we can expect the errors in atomization energies to be between those for DFA and PZSIC-DFA errors. This trend can be seen in Table II.

Additionally, we studied the 37 molecules used in our earlier work (Ref. 88). We experienced SCF convergence issues with the vSOSIC approach for LiBr and NaBr with Jacobi rotation when a large core SOSIC treatment is used on the bromine atom. In such cases, using small core SOSIC can eliminate the issues.

The qualitative performance of vSOSIC using a small core for the larger atoms is summarized in Table II compared against Ref. 119. The trends in atomization energies for the AE6 and the larger set are similar for LSDA in that the MAEs are reduced with PZSIC-LSDA compared to DFA-LSDA. With PBE and r<sup>2</sup>SCAN functionals, the MAEs for the larger set are comparable with the three approaches. On the other hand, with AE6 set, the application of SIC introduces large errors with r<sup>2</sup>SCAN. Since AE6 is a small set, the larger set is more likely to show the general performance of these functionals. Overall, the vSOSIC-DFA MAEs are close to those of PZSIC-DFAs.

## B. Barrier heights

The barrier heights of chemical reactions are difficult to describe correctly with a DFA since the SIE appears in stretched bond situations at the saddle point calculation. DFAs due to SIEs tend to incorrectly provide lower energies for the transition states. Previously, PZSIC performance on the BH76 set was studied<sup>121</sup>, and it is reported that both accurate energy functional as well as accurate electron density are important for describing barrier height calculations. Furthermore, previous SOSIC work<sup>75</sup> on the reaction barrier heights of the BH6 dataset<sup>118</sup> showed that SOSIC works well when it includes only the orbitals corresponding to the stretched bonds.

Here, we systematically compare the performance of the vSOSIC methods on reaction barrier heights using the BH6 set. The reactions of BH6 are (a)  $\text{OH} + \text{CH}_4 \rightarrow \text{CH}_3 + \text{H}_2\text{O}$ , (b)  $\text{H} + \text{OH} \rightarrow \text{H}_2 + \text{O}$ ,

and (c)  $\text{H} + \text{H}_2\text{S} \rightarrow \text{H}_2 + \text{HS}$ . There are six barrier heights from the combined forward and reverse reaction pathways. Table III provides a summary of the results and shows that vSOSIC performance is nearly identical to that of PZSIC with comparable MAEs for the three functionals.

Since the BH6 set is a rather small set of reaction barriers, we also additionally used the WCPT18 set<sup>122</sup> to evaluate the vSOSIC performance in comparison to PZSIC. The WCPT18 set consists of 18 reaction barrier heights and requires 28 single-point calculations. The set consists of 9 water-catalyzed proton-transfer reactions that involve zero, one, or two water molecules as a catalyst. The MAEs of the WCPT18 set presented in Table III for LSDA, PBE and r<sup>2</sup>SCAN show that the vSOSIC and PZSIC results agree within 1 kcal/mol. This is expected since the proton transfer reactions involve stretching electron density on the hydrogen atom where SIC is truly needed. This stretching happens on valence orbitals, where vSOSIC and PZSIC have the same SIC effect on these orbitals.

## C. Highest occupied molecular orbital eigenvalues for 38 selected molecules

Janak’s theorem relates that the negative of the highest occupied molecular orbital (HOMO) eigenvalue in DFT is equivalent to the vertical ionization potential (IP)<sup>123–126</sup>. Since many DFAs do not have a correct asymptotic potential character, their exchange-correlation potentials tend to be too shallow in the asymptotic region, resulting thereby in absolute HOMO eigenvalues that underestimate the IPs. PZSIC is shown to lower the HOMO energy levels by deepening the exchange-correlation potential and widening the HOMO-LUMO gaps. This usually results in a much-improved agreement between absolute of HOMO eigenvalues with experimental IPs or higher-level theories.

Fig. 4 compares the difference of absolute of HOMO eigenvalues of the 38 molecules that are a subset of G2/97 set and experimental IP for PZSIC-DFA and vSOSIC-DFA for LSDA, PBE, and r<sup>2</sup>SCAN. Although absolute HOMO eigenvalues in PZSIC estimate IPs better than DFA, the absolute HOMO eigenvalues of PZSIC overestimate the experimental IPs by up to 4 eV for the set of molecules studied here. vSOSIC HOMO eigenvalues are in good agreement with PZSIC. The eigenvalue spectra of LiBr and NaBr molecules are shown in Supplementary Materials where it can be seen that SOSIC and PZSIC valence eigenvalues are essentially identical.

TABLE II: Mean absolute error (MAE) in kcal/mol and mean absolute percentage error (MAPE) in % of atomization energy for the data sets AE6 and 37-molecules.<sup>a b</sup>

Functional	Method	MAE(kcal/mol)		MAPE(%)	
		AE6	37-molecules	AE6	37-molecules
LSDA	DFA	74.3 <sup>a</sup>	64.5	15.9 <sup>a</sup>	24.2 <sup>b</sup>
LSDA	PZSIC	58.0 <sup>a</sup>	46.8 <sup>b</sup>	9.4 <sup>a</sup>	13.4 <sup>b</sup>
LSDA	vSOSIC	66.6	51.1	11.0	13.8
PBE	DFA	13.4 <sup>a</sup>	23.7 <sup>b</sup>	3.3 <sup>a</sup>	8.6 <sup>b</sup>
PBE	PZSIC	18.8 <sup>a</sup>	20.2 <sup>b</sup>	6.8 <sup>a</sup>	9.7 <sup>b</sup>
PBE	vSOSIC	16.3	22.7	5.3	9.6
r <sup>2</sup> SCAN	DFA	3.0	16.0	1.9	6.1
r <sup>2</sup> SCAN	PZSIC	26.3	16.7	6.9	9.9
r <sup>2</sup> SCAN	vSOSIC	17.2	17.1	5.1	8.9

<sup>a</sup> Reference 120

<sup>b</sup> Reference 88

TABLE III: Mean absolute error (MAE) in kcal/mol for the reaction barrier heights of BH6 and WCPT18 sets.

Functional	Method	MAE(kcal/mol)	
		BH6	WCPT18
LSDA	DFA	17.6 <sup>a</sup>	17.7
LSDA	PZSIC	4.9 <sup>a</sup>	7.5
LSDA	vSOSIC	5.2	7.6
PBE	DFA	8.0 <sup>a</sup>	8.8
PBE	PZSIC	4.2 <sup>a</sup>	10.3
PBE	vSOSIC	4.1	9.4
r <sup>2</sup> SCAN	DFA	7.6	6.2
r <sup>2</sup> SCAN	PZSIC	2.8	6.0
r <sup>2</sup> SCAN	vSOSIC	2.6	5.5

<sup>a</sup>Reference 120

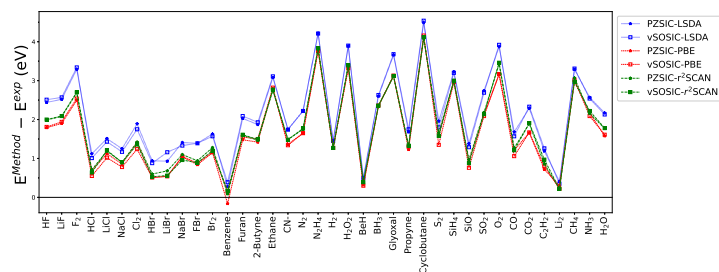


FIG. 4: Negative of HOMO eigenvalues of 38 selected molecules, a subset of G2/97 set, compared against experimental ionization potential for three functionals and two SIC methods.

#### D. Vertical detachment energy of water cluster anions

Electron hydration is an important phenomenon in biological processes.<sup>127,128</sup> Modeling such behavior is challenging for the local and semi-local DFA. The semi-local GGA and meta-GGA and B3LYP performance are rather poor for such systems as the electron attached to the water cluster is delocalized over the system. Typically, the extent of the delocalization worsens with increasing water cluster size, and consequently, post-Hartree-Fock methods are often the methods of choice. Recent studies by Vargas and coworkers showed that SIC methods can be a good alternative to Møller-Plesset second-order perturbation theory (MP2) and LC-BOP level of the-

ory for describing the systems of hydrated electrons.<sup>98</sup> An excess electron in water clusters can be dipole-bound, trapped on a cluster surface, solvated internally to a cluster, or bound to dangling OH bonds of a cluster.<sup>112</sup> In all situations, active orbitals play an important role. Earlier studies carried out by this group on electron binding to water clusters have shown that PZSIC-PBE can predict the vertical detachment energies (VDE) in comparable accuracy as the CCSD(T) level of theory when the negative of the HOMO eigenvalue is used to estimate VDE. To assess the present SOSIC approach, we have computed the vertical detachment energies of water clusters from the absolute of the HOMO eigenvalues with only the PBE functional. We consider water dimer, five trimers (3AAa, 3Da, 3I-1a, 3I-2a, and 3La), four tetramers (4AAa, 4Da, 4Ia, and 4La), five pentamers (5AA-1a, 5AA-2a, 5Da, 5Ia, and 5La), and five hexamers (6AA-1a, 6AA-2a, 6Da, 6Ia, and 6La). The same isomer notation is used as in the references 98 and 112.

The calculated VDEs are shown in Table IV where PZSIC-PBE, vSOSIC-PBE, and CCSD(T) values from Ref. 112 are compared. The vSOSIC-PBE performance is very close to PZSIC-PBE with MAEs of 16.9 (PZSIC-PBE) and 15.0 meV (vSOSIC-PBE) when compared to CCSD(T) values, respectively. The differences between the PZSIC-PBE and vSOSIC-PBE VDE values are 20 meV or less for the majority of the isomers except for 6AA-1a for which the difference is 53 meV.

Typically, the extra electron in water cluster anions is unbound in the standard DFA calculations with positive HOMO eigenvalues. As demonstrated above, the vSOSIC-PBE and PZSIC-PBE can accurately describe electron binding in these clusters. Thus, the removal of SIE from the valence orbitals can cure the failure of DFAs. As an interesting application of vSOSIC, here we further examine if removing the SIE for just one orbital (the last orbital with the extra electron) can improve the description of electron binding in these clusters. The results of this one-orbital SOSIC show that the removal of SIE from just one orbital results in electron binding with negative HOMO eigenvalues for all the clusters. In this case, the VDEs obtained from the HOMO eigenvalues however show a higher MAE of 56.9 meV. Although this MAE is larger compared to the all orbital PZSIC-PBE, it is still comparable to MP2 MAE (44 meV) and far better than that of B3LYP (238 meV)<sup>98</sup>. It is remarkable that the removal of SIE from just one orbital (extra electron) can result in a major improvement in the VDEs of water anions since the cost of this calculation is practically the same as that of PBE functional. Since the SIC is applied only to the extra electron, the FLO in this case is same as the Kohn-Sham orbital. This approach therefore can be readily introduced in most density functional codes.

TABLE IV: Vertical detachment energy of water cluster anions is estimated as the absolute values of the HOMO eigenvalues. MAE (in meV) is calculated with respect to CCSD(T) from Reference 112.

System	PZSIC-PBE	vSOSIC-PBE	1orb-SOSIC-PBE	CCSD(T) <sup>a</sup>
2La	30	33	18	29
3AAa	180	184	149	187
3Da	14	17	4	6
3I-1a	205	216	107	190
3I-2a	185	188	146	175
3La	148	156	129	146
4AAa	314	319	279	336
4Da	42	62	41	49
4Ia	456	445	314	439
4La	236	246	216	255
5AA-1a	358	385	294	370
5AA-2a	354	357	315	376
5Da	73	77	54	61
5Ia	467	473	372	469
5La	277	282	254	294
6AA-1a	521	574	425	553
6AA-2a	443	456	392	477
6Da	114	118	87	104
6Ia	904	891	671	839
6La	358	367	331	381
MAE	16.9	15.0	56.9	

<sup>a</sup> Reference 112

## E. Magnetic exchange coupling constant of chlorocuprate

The magnetic exchange interaction between localized spins is another property what is affected by the delocalization error arising from the SIE in the DFAs. The coupling strength between two magnetic spins is characterized by a quantity known as magnetic exchange coupling constant ( $J$ ), and its sign and magnitude determine the magnetic nature and strength of materials. The spin Hamiltonian for such interaction is written as

$$H_{spin} = -J \sum_{i,j} \mathbf{S}_i \cdot \mathbf{S}_j. \quad (7)$$

By relating the DFT energy of high-spin and low-spin states with a given electron configuration to the  $H_{spin}$  of the corresponding spin configuration, we can determine the value of  $J$  from the DFT calculations. As an application of the vSOSIC method, we compute the magnetic exchange coupling constant of  $[\text{Cu}_2\text{Cl}_6]^{2-}$  system and compare the results with previous SIC results by Mishra *et al.* and other groups.<sup>80,81,129,130</sup> With LSDA and PBE, the coupling strength

TABLE V: Magnetic exchange coupling constant  $J$  in  $\text{cm}^{-1}$  for hexachlorocuprate  $[\text{Cu}_2\text{Cl}_6]^{2-}$  at planar  $\theta = 0^\circ$ .

Method	$J$
PZSIC-LSDA	-78 <sup>a</sup>
vSOSIC-LSDA	-84
LSDA@PZSIC-LSDA	-131 <sup>a</sup>
LSDA@vSOSIC-LSDA	-137
PZSIC-PBE	-94 <sup>a</sup>
vSOSIC-PBE	-84
PBE@PZSIC-PBE	-138 <sup>a</sup>
PBE@vSOSIC-PBE	-124
PZSIC-r <sup>2</sup> SCAN	-77 <sup>b</sup>
vSOSIC-r <sup>2</sup> SCAN	-93
Exp.	0 to -40 <sup>c</sup>

<sup>a</sup> Reference 81 where the values are calculated with an ECP approach for the PZSIC method.

<sup>b</sup> ECP was used in the calculation.

<sup>c</sup> Reference 132

of this molecule is overestimated by a few orders. Previous PZSIC studies<sup>81</sup> using ECP showed that both the SIC correction to the energy and to the density are needed for accurate descriptions of coupling constants with LSDA and PBE functionals. On the other hand, for the SCAN family of functionals, **sometimes** only SIC correction to the density may be sufficient.<sup>88,96</sup>

The magnetic exchange coupling constant is computed using the spin projection approach of Noodleman<sup>131</sup> given as a formula,  $J = (E_{BS} - E_{HS}) / (2S_A S_B)$ , where  $S_A$  and  $S_B$  are the spins at two magnetic centers, A and B.  $E_{BS}$  is the energy of the molecule in broken symmetry spin configuration ( $\uparrow\downarrow$ ) and  $E_{HS}$  is energy in high-spin configuration ( $\uparrow\uparrow$ ). The vSOSIC calculated magnetic exchange coupling constants are compared with previous results in Table V. It is evident that the two methods (PZSIC and vSOSIC) differ at most by  $10 \text{ cm}^{-1}$  for the LSDA and PBE functionals. We note that the magnetic exchange coupling constant is more sensitive to the accuracy in the total energies than other non-magnetic properties, and it requires tighter convergence criteria in FOD optimizations than usual calculations. The density-corrected DFA is a good way to improve the DFA predictions when DFA errors are suspected to be due to density delocalization errors. By comparing both DFA@PZSIC-DFA and DFA@vSOSIC-DFA, we find that the difference is 6 and  $14 \text{ cm}^{-1}$  for LSDA and PBE cases, respectively.

## F. Spin charges in square planar copper complexes

As the final case study, we applied the vSOSIC method to the square planar copper molecule previously studied by Karanovich *et al.*<sup>85</sup>. They analyzed the electronic configurations for monoanionic  $[\text{Cu}(\text{C}_6\text{H}_4\text{S}_2)_2]^-$  (Q1) and dianionic  $[\text{Cu}(\text{C}_6\text{H}_4\text{S}_2)_2]^{2-}$  (Q2) Cu-based molecules. Similar magnetic square planar structures  $[\text{Cu}(\text{C}_{14}\text{H}_{20}\text{S}_2)_2]^z$  ( $z = 2-, 1-, 0$ ) are synthesized experimentally.<sup>133</sup> Due to its long spin-lattice relaxation times,  $[\text{Cu}(\text{C}_{14}\text{H}_{20}\text{S}_2)_2]^{2-}$  complex is considered as a candidate for qubits in the area of quantum information science. There has been a debate about the electronic structures of these square planar metal structures, and it has been suggested that beyond-DFT methods such as multireference methods or potentially SIC methods may be required to study these complexes.<sup>85,133–135</sup> Use of popular functionals such as PBE or B3LYP results in incorrect electron delocalization for the copper d-electrons. The Mulliken spin population at the Cu site with PBE is  $0.32 \mu_B$ , compared to the EPR experimental value of  $0.51 \mu_B$ . PZSIC-LSDA yields  $0.67 \mu_B$ , which is more similar to the Hartree-Fock and CASSCF estimates ( $0.79$  and  $0.70 \mu_B$ , respectively).<sup>85</sup> The PZSIC tendency to overestimate the spin population has also been observed in spin-crossover complexes<sup>83</sup>. Within the PBE and B3LYP functionals, the HOMO energy for the Q2 complex is positive, indicating that the additional electron is not bound to the complex. In both complexes, HOMO energy decreases from PBE to PZSIC-LSDA by 4.6 and 5.0 eV for Q1 and Q2 complexes, respectively. The HOMO and LUMO eigenvalues and spin population obtained with vSOSIC are presented in Table VI. Both the PZSIC-LSDA and vSOSIC-LSDA HOMO energies are negative and agree within 0.1 eV. Similarly, the difference in Mulliken spin population between PZSIC and vSOSIC is  $0.12 \mu_B$  and  $0.01 \mu_B$  for the Cu and S atoms in Q2. The spin population for Q1 is excluded from the table since their spin moment is zero. In this SOSIC calculation, 100 orbitals out of 175 total orbitals are treated with SIC reducing the computation time by 57%. The reduced FOD structure for the vSOSIC method is shown in Fig. 1. PZSIC calculations on transition metal complexes surrounded by ligands are often computationally costly. These systems demonstrate how vSOSIC can be significantly more computationally efficient than PZSIC.

## IV. EFFICIENCY OF VSOSIC METHOD

As a reminder, PZSIC is a one-electron SIC approach wherein self-interaction correction is obtained in an orbital-by-orbital fashion. Thus, a rough estimate of the computational cost of PZSIC calculation is approximately  $N + 1$  times more than a DFA calculation,  $N$  is the number of electrons in the system. The actual cost



TABLE VI: The Mulliken population on the Cu and all four S atoms and HOMO and LUMO eigenvalues of (Q1)  $[\text{Cu}(\text{C}_6\text{H}_4\text{S}_2)_2]^{1-}$  and (Q2)  $[\text{Cu}(\text{C}_6\text{H}_4\text{S}_2)_2]^{2-}$ .

System	Method	Mulliken population ( $\mu_B$ )		HOMO (eV)	LUMO (eV)	No. SIC orbitals
		Cu	S			
Q1	PZSIC-LSDA			-5.9	-1.2	174
	SOSIC-LSDA			-5.9	-1.4	100
Q2	PZSIC-LSDA	0.67	0.33	-2.0	4.4	175
	SOSIC-LSDA	0.55	0.34	-1.9	4.1	101

of calculation can be much higher than this estimate since localized orbital densities need to be determined. In the FLOSIC method, this amounts to the optimization of FODs that determine the FLOs used to evaluate SIC terms. Our experience shows that the FOD energy surface is often very shallow with multiple minima, and typically the FODs corresponding to the core orbitals, especially the 1s orbital, are harder to optimize. Such problems make the FLOSIC calculations time-consuming. Thus, by applying SIC to select orbitals, computational costs can be substantially reduced.

vSOSIC can accelerate SIC computations in two ways. As done in this work, with only the valence orbitals the vSOSIC calculation for a given set of FODs is  $(N+1)/(N-N_{core}+1)$  times faster compared to a regular PZSIC calculation. Here  $N_{core}$  and  $N$  are the number of core orbitals and total orbitals, respectively. This also results in having to optimize  $3(N-N_{core})$  FOD parameters in vSOSIC instead the  $3N$  in the PZSIC. As mentioned earlier, the optimization of the core FOD parameters is often unsteady, and their removal usually leads to smoother optimization in vSOSIC.

As an illustration of computational savings, we consider the  $[\text{Cu}_2\text{Cl}_6]^{2-}$  complex and perform vSOSIC and PZSIC with LSDA functional calculations on the NERSC Perlmutter supercomputer that is equipped with AMD EPYC 7763 CPU with base (max) clock speed 2.45GHz (3.5GHz). We utilized two CPU sockets, resulting in a total of 128 cores per node. For conducting the timing test, only one node was used. The number of electrons treated with SIC in PZSIC (vSOSIC) is 160 (80), and a single iteration step takes 343.4 (174.6) seconds with the above setup. This speedup in an SCF from PZSIC to SOSIC is in agreement with the expected speedup of  $(N+1)/(N-N_{core}+1) \approx 2$ . In Fig. 5 (a) we show the relative energy with respect to their converged energies as a function of FOD update steps for the same system. The FOD optimization in PZSIC requires  $\approx 105$  steps to reach the final energy within  $10^{-4} E_h$  (where the tolerance in the energy derivative is  $10^{-2} E_h/a_0$ ). In the vSOSIC, the relative energy, as well as the energy derivative, is almost one order lower than the PZSIC at the same FOD update step.

The largest component of FOD force is plotted as a function of

update steps in Fig. 5 (b). For this system, in the PZSIC method force drops below  $10^{-2} E_h/a_0$  after around 45 steps whereas in the vSOSIC method it takes only 10 steps. The vSOSIC method is advantageous in FOD optimization.

## V. SUMMARY AND OUTLOOK

We have outlined and assessed a simplified one-electron self-interaction-correction scheme where the SIE is removed from a select set of orbitals. In this work, the set chosen is valence orbitals since it is the valence orbitals that define central aspects of the electronic structure and chemical bonding. The approach is, however, more general and can also be used to correct for core states if needed, for example, in the computation of core-electron binding energies. It can also be adapted to apply SIC to a specific region of space, as in the spirit of embedding methods, by identifying the FLOs that are localized in the region of interest. The present vSOSIC approach differs from the SOSIC method introduced in Ref. 75 in that the Fermi-Löwdin orbitals that are used in evaluating the SIC are constructed from the valence Kohn-Sham orbitals only. This results in a substantial reduction in the computational complexities by reducing the number of Fermi orbital descriptors that need to be optimized thereby providing significant computational speed up. The results obtained using the vSOSIC scheme are compared with those obtained with PZSIC which corrects for all the orbitals. We have studied the performance of vSOSIC on the total energies of atoms, atomization energies, reaction barrier heights, and HOMO eigenvalues of molecules. For the atomization energies of AE6 datasets, with the LSDA functionals MAE with vSOSIC MAE is larger by 7 kcal/mol than the PZSIC, for the PBE functionals vSOSIC MAE is 2 kcal/mol lower while for the r<sup>2</sup>SCAN functional vSOSIC MAE is 9 kcal/mol smaller than that of PZSIC. These differences between the performance of vSOSIC and PZSIC diminish for a larger dataset (37 molecules from the MGAE109). The vSOSIC and PZSIC perform similarly within 0.2 kcal/mol in

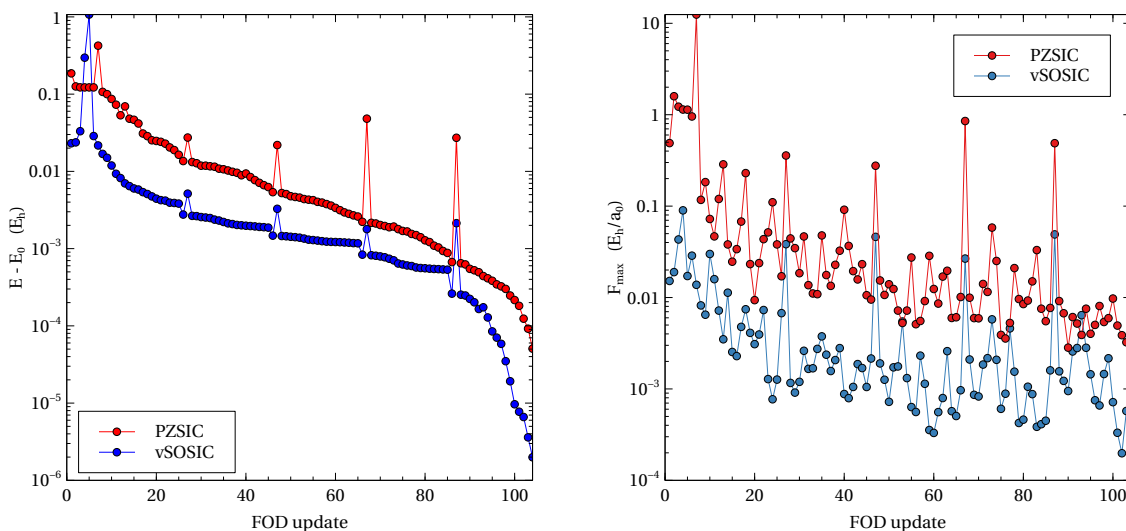


FIG. 5: PZSIC and vSOSIC for the relative total energies with respect to their final converged energies as a function of the FOD update steps (left pane) and the largest FOD force component as a function of the FOD update (right pane).

the calculation of the barrier heights of BH6 and WCPT18 datasets. Likewise, the absolute HOMO eigenvalues that approximate the vertical ionization energies, obtained by the vSOSIC and PZSIC are in excellent agreement with each other but they both overestimate the experimental ionization energies. Furthermore, we applied vSOSIC to VDEs of water cluster anions, and magnetic exchange coupling parameters of  $[\text{Cu}_2\text{Cl}_6]^{2-}$  and electronic structure of  $[\text{Cu}(\text{C}_6\text{H}_4\text{S}_2)_2]^{1-/2-}$  as a test on systems containing transition metals. The vSOSIC and PZSIC predicted exchange coupling constants differ by 6 and 10  $\text{cm}^{-1}$  for the LSDA and PBE functionals, respectively. For the  $[\text{Cu}(\text{C}_6\text{H}_4\text{S}_2)_2]^{1-/2-}$  molecules, the vSOSIC like PZSIC binds the extra electrons and yields HOMO eigenvalues within 0.1 eV of PZSIC, while for the spin-moment at Cu site, vSOSIC prediction ( $0.55 \mu_B$ ) agrees with PZSIC ( $0.67 \mu_B$ ) within  $0.1 \mu_B$  with vSOSIC value being closer to the EPR experimental value of  $0.51 \mu_B$ . The water cluster anions offer an interesting case. Our previous work with PZSIC-PBE showed that the negative of the highest occupied eigenvalue offered an outstanding approximation to the VDE of the water cluster anions, with an MAE of only 17 meV when compared to CCSD(T) values. These results outperformed MP2 method and other hybrid functionals by a wide margin. The vSOSIC technique (with PBE functional) decreases the MAE by another 2 meV, making it an ideal alternative to CCSD(T) for determining the VDE of water cluster anions. To determine the VDE of the water anions, an even more straightforward form of SOSIC was explored, in which just the outermost unpaired or-

bital was corrected for SIE. Interestingly in this scheme, we find that the HOMO eigenvalue is negative indicating electron binding. However, the VDEs derived from the HOMO eigenvalues, in this case, exhibit a higher MAE of 56.9 meV, which is still superior to B3LYP (238 meV) and comparable to MP2 MAE (44 meV). These 1orb-SOSIC results are highly encouraging because the computing cost is nearly the same as that of the uncorrected density functional technique making 1orb-SOSIC useful in molecular dynamics simulations of such complexes. The vSOSIC calculations on the  $[\text{Cu}_2\text{Cl}_6]^{2-}$  complex as an instructive example of the computational efficiency demonstrates that, in addition to the savings from using fewer orbitals to account for SIC, the FOD optimization in vSOSIC is substantially smoother and quicker. Overall, the vSOSIC method involves fewer calculations than the PZSIC method and produces results similar to the PZSIC method. As seen in the computation of the VDE of water anions, the approach may be tailored to the task at hand by selecting relevant orbitals for SIE removal. For example, the properties related to the core orbitals such as core electron binding energies, or Fermi-contact terms will require different choices of the active orbitals in the SOSIC method. The vSOSIC approach can be particularly useful for studying a large complex composed of heavy elements where SIC effects are expected to be more pronounced due to localized f-electrons.

This work also assessed the performance of the  $r^2\text{SCAN}$  functional with PZSIC and vSOSIC methods for a range of properties. Our results show that SIC- $r^2\text{SCAN}$  calculations require about 2-

3 times fewer grid points than the SIC-SCAN calculations. SIC- $r^2$ SCAN performs similarly to the SIC-SCAN for most properties but for atomization energies, SIC- $r^2$ SCAN outperforms SIC-SCAN, which is the opposite of the tendency seen with uncorrected functionals.

## DATA AVAILABILITY STATEMENT

The data that support the findings of this study are available within the article and its supplementary material.

## ACKNOWLEDGEMENT

This work was supported by the U.S. Department of Energy, Office of Science, Office of Basic Energy Sciences, as part of the Computational Chemical Sciences Program under Award No. DE-SC0018331. Support for computational time at the Texas Advanced Computing Center (TACC), the Advanced Cyberinfrastructure Coordination Ecosystem: Services & Support (ACCESS) program, and the National Energy Research Scientific Computing Center (NERSC) is gratefully acknowledged.

- <sup>1</sup>W. Kohn and L. Sham, "Self-consistent equations including exchange and correlation effects," *Phys. Rev.* **140**, A1133–A1138 (1965).
- <sup>2</sup>M. Levy, "Universal variational functionals of electron densities, first-order density matrices, and natural spin-orbitals and solution of the  $v$ -representability problem," *Proceedings of the National Academy of Sciences* **76**, 6062–6065 (1979).
- <sup>3</sup>A. Fouda and U. Ryde, "Does the DFT self-interaction error affect energies calculated in proteins with large QM systems?" *J. Chem. Theory Comput.* **12**, 5667–5679 (2016).
- <sup>4</sup>E. R. Johnson, A. Otero-de-la Roza, and S. G. Dale, "Extreme density-driven delocalization error for a model solvated-electron system," *J. Chem. Phys.* **139**, 184116 (2013), <https://doi.org/10.1063/1.4829642>.
- <sup>5</sup>L. M. LeBlanc, S. G. Dale, C. R. Taylor, A. D. Becke, G. M. Day, and E. R. Johnson, "Pervasive delocalisation error causes spurious proton transfer in organic acid–base Co-crystals," *Angew. Chem. Int. Ed.* **130**, 15122–15126 (2018).
- <sup>6</sup>J. Autschbach and M. Srebro, "Delocalization error and "functional tuning" in Kohn–Sham calculations of molecular properties," *Acc. Chem. Res.* **47**, 2592–2602 (2014).
- <sup>7</sup>B. Rana, M. P. Coons, and J. M. Herbert, "Detection and correction of delocalization errors for electron and hole polarons using density-corrected DFT," *J. Phys. Chem. Lett.* **13**, 5275–5284 (2022).
- <sup>8</sup>X. A. Sosa Vazquez and C. M. Isborn, "Size-dependent error of the density functional theory ionization potential in vacuum and solution," *J. Chem. Phys.* **143**, 244105 (2015).
- <sup>9</sup>I. Lindgren, "A statistical exchange approximation for localized electrons," *Int. J. Quantum Chem.* **5**, 411–420 (1971).
- <sup>10</sup>J. Perdew, "Orbital functional for exchange and correlation: self-interaction correction to the local density approximation," *Chem. Phys. Lett.* **64**, 127–130 (1979).
- <sup>11</sup>J. P. Perdew and A. Zunger, "Self-interaction correction to density-functional approximations for many-electron systems," *Phys. Rev. B* **23**, 5048–5079 (1981).
- <sup>12</sup>U. Lundin and O. Eriksson, "Novel method of self-interaction corrections in density functional calculations," *Int. J. Quantum Chem.* **81**, 247–252 (2001).
- <sup>13</sup>M. S. Gopinathan, "Improved approximate representation of the Hartree-Fock potential in atoms," *Phys. Rev. A* **15**, 2135–2142 (1977).
- <sup>14</sup>A. Zunger, J. Perdew, and G. Oliver, "A self-interaction corrected approach to many-electron systems: Beyond the local spin density approximation," *Solid State Commun.* **34**, 933–936 (1980).
- <sup>15</sup>O. Gunnarsson and R. O. Jones, "Self-interaction corrections in the density functional formalism," *Solid State Commun.* **37**, 249–252 (1981).
- <sup>16</sup>S. Manoli and M. Whitehead, "Generalized-exchange local-spin-density-functional theory: Self-interaction correction," *Phys. Rev. A* **38**, 630 (1988).
- <sup>17</sup>Y. Guo and M. Whitehead, "An alternative self-interaction correction in the generalized exchange local-density functional theory," *J. Comput. Chem.* **12**, 803–810 (1991).
- <sup>18</sup>M. R. Pederson, R. A. Heaton, and C. C. Lin, "Local-density Hartree-Fock theory of electronic states of molecules with self-interaction correction," *J. Chem. Phys.* **80**, 1972–1975 (1984), <https://doi.org/10.1063/1.446959>.
- <sup>19</sup>M. R. Pederson, R. A. Heaton, and C. C. Lin, "Density-functional theory with self-interaction correction: Application to the lithium molecule," *J. Chem. Phys.* **82**, 2688–2699 (1985), <https://doi.org/10.1063/1.448266>.
- <sup>20</sup>J. Harrison, R. Heaton, and C. Lin, "Self-interaction correction to the local density Hartree-Fock atomic calculations of excited and ground states," *J. PHYS. B-AT MOL. OPT.* **16**, 2079 (1983).
- <sup>21</sup>J. G. Harrison, "An improved self-interaction-corrected local spin density functional for atoms," *J. Chem. Phys.* **78**, 4562–4566 (1983).
- <sup>22</sup>R. A. Heaton and C. C. Lin, "Self-interaction-correction theory for density functional calculations of electronic energy bands for the lithium chloride crystal," *J. Phys. C Solid State Phys.* **17**, 1853–1866 (1984).
- <sup>23</sup>R. A. Heaton and C. C. Lin, "Electronic energy-band structure of the calcium fluoride crystal," *Phys. Rev. B* **22**, 3629 (1980).
- <sup>24</sup>H. Gudmundsdottir, E. Ö. Jónsson, and H. Jónsson, "Calculations of Al dopant in  $\alpha$ -quartz using a variational implementation of the Perdew–Zunger self-interaction correction," *New J. Phys.* **17**, 083006 (2015).
- <sup>25</sup>E. Ö. Jónsson, S. Lehtola, and H. Jónsson, "Towards an optimal gradient-dependent energy functional of the PZ-SIC form," *Procedia Comput. Sci.* **51**, 1858–1864 (2015).
- <sup>26</sup>S. Lehtola, E. O. Jónsson, and H. Jónsson, "Effect of complex-valued optimal orbitals on atomization energies with the Perdew–Zunger self-interaction correction to density functional theory," *J. Chem. Theory Comput.* **12**, 4296–4302 (2016).
- <sup>27</sup>S. Klüpfel, P. Klüpfel, and H. Jónsson, "The effect of the perdew-zunger self-interaction correction to density functionals on the energetics of small molecules," *J. Chem. Phys.* **137**, 124102 (2012).
- <sup>28</sup>S. Lehtola and H. Jónsson, "Variational, self-consistent implementation of the Perdew–Zunger self-interaction correction with complex optimal orbitals," *J. Chem. Theory Comput.* **10**, 5324–5337 (2014).
- <sup>29</sup>O. A. Vydrov and G. E. Scuseria, "Ionization potentials and electron affinities in the perdew–zunger self-interaction corrected density-functional theory," *J. Chem. Phys.* **122**, 184107 (2005).
- <sup>30</sup>O. A. Vydrov and G. E. Scuseria, "Effect of the Perdew–Zunger self-interaction correction on the thermochemical performance of approximate density functionals," *J. Chem. Phys.* **121**, 8187–8193 (2004).
- <sup>31</sup>S. Lehtola, M. Head-Gordon, and H. Jónsson, "Complex orbitals, multiple local minima, and symmetry breaking in Perdew–Zunger self-interaction corrected density functional theory calculations," *J. Chem. Theory Comput.* **12**, 3195–3207 (2016).
- <sup>32</sup>B. G. Janesko, "Systematically improvable generalization of self-interaction corrected density functional theory," *J. Phys. Chem. Lett.* **13**, 5698–5702 (2022).

- <sup>33</sup>E. J. Bylaska, K. Tsemekhman, and F. Gao, “New development of self-interaction corrected DFT for extended systems applied to the calculation of native defects in 3C–SiC,” *Phys. Scr.* **2006**, 86 (2006).
- <sup>34</sup>A. Ruzsinszky, J. P. Perdew, G. I. Csonka, O. A. Vydrov, and G. E. Scuseria, “Density functionals that are one- and two- are not always many-electron self-interaction-free, as shown for  $H_2^+$ ,  $He_2^+$ ,  $LiH^+$ , and  $Ne_2^+$ ,” *J. Chem. Phys.* **126**, 104102 (2007), <https://doi.org/10.1063/1.2566637>.
- <sup>35</sup>A. Ruzsinszky, J. P. Perdew, G. I. Csonka, O. A. Vydrov, and G. E. Scuseria, “Spurious fractional charge on dissociated atoms: Pervasive and resilient self-interaction error of common density functionals,” *J. Chem. Phys.* **125**, 194112 (2006), <https://doi.org/10.1063/1.2387954>.
- <sup>36</sup>K. A. Jackson, J. E. Peralta, R. P. Joshi, K. P. Withanage, K. Trepte, K. Sharkas, and A. I. Johnson, “Towards efficient density functional theory calculations without self-interaction: The Fermi–Löwdin orbital self-interaction correction,” *J. Phys. Conf. Ser.* **1290**, 012002 (2019).
- <sup>37</sup>S. Patchkovskii and T. Ziegler, “Improving “difficult” reaction barriers with self-interaction corrected density functional theory,” *J. Chem. Phys.* **116**, 7806–7813 (2002).
- <sup>38</sup>S. Kümmel and J. P. Perdew, “Two avenues to self-interaction correction within Kohn–Sham theory: Unitary invariance is the shortcut,” *Mol. Phys.* **101**, 1363–1368 (2003).
- <sup>39</sup>T. Körzdörfer, S. Kümmel, and M. Mundt, “Self-interaction correction and the optimized effective potential,” *J. Chem. Phys.* **129**, 014110 (2008).
- <sup>40</sup>T. Baruah, R. R. Zope, A. Kshirsagar, and R. K. Pathak, “Positron binding: A positron-density viewpoint,” *Phys. Rev. A* **50**, 2191–2196 (1994).
- <sup>41</sup>V. Polo, E. Kraka, and D. Cremer, “Electron correlation and the self-interaction error of density functional theory,” *Mol. Phys.* **100**, 1771–1790 (2002).
- <sup>42</sup>R. A. Heaton, J. G. Harrison, and C. C. Lin, “Self-interaction correction for density-functional theory of electronic energy bands of solids,” *Phys. Rev. B* **28**, 5992–6007 (1983).
- <sup>43</sup>S. Goedecker and C. Umrigar, “Critical assessment of the self-interaction-corrected–local-density-functional method and its algorithmic implementation,” *Physical Review A* **55**, 1765 (1997).
- <sup>44</sup>A. Svane, “Electronic structure of cerium in the self-interaction-corrected local-spin-density approximation,” *Phys. Rev. B* **53**, 4275–4286 (1996).
- <sup>45</sup>A. Svane, W. M. Temmerman, Z. Szotek, J. Lægsgaard, and H. Winter, “Self-interaction-corrected local-spin-density calculations for rare earth materials,” *Int. J. Quantum Chem.* **77**, 799–813 (2000).
- <sup>46</sup>M. M. Rieger and P. Vogl, “Self-interaction corrections in semiconductors,” *Phys. Rev. B* **52**, 16567–16574 (1995).
- <sup>47</sup>R. R. Zope, M. K. Harbola, and R. K. Pathak, “Atomic Compton profiles within different exchange-only theories,” *Eur. Phys. J. D-AMOP Phys.* **7**, 151–155 (1999).
- <sup>48</sup>N. Hamada and S. Ohnishi, “Self-interaction correction to the local-density approximation in the calculation of the energy band gaps of semiconductors based on the full-potential linearized augmented-plane-wave method,” *Phys. Rev. B* **34**, 9042 (1986).
- <sup>49</sup>M. Biagini, “Self-interaction-corrected density-functional formalism,” *Phys. Rev. B* **49**, 2156 (1994).
- <sup>50</sup>Y. Xie, R. Han, and X. Zhang, “Obtaining localized orbitals and band structure in self-interaction-corrected density-functional theory,” *Phys. Rev. B* **60**, 8543 (1999).
- <sup>51</sup>M. Arai and T. Fujiwara, “Electronic structures of transition-metal mono-oxides in the self-interaction-corrected local-spin-density approximation,” *Phys. Rev. B* **51**, 1477 (1995).
- <sup>52</sup>M. Stengel and N. A. Spaldin, “Self-interaction correction with Wannier functions,” *Phys. Rev. B* **77**, 155106 (2008).
- <sup>53</sup>D. L. Price, “Application of an on-site self-interaction-corrected method to Ce and the  $\alpha$ -Ce surface,” *Phys. Rev. B* **60**, 10588 (1999).
- <sup>54</sup>C. Legrand, E. Suraud, and P. Reinhard, “Comparison of self-interaction-corrections for metal clusters,” *Journal of Physics B: Atomic, Molecular and Optical Physics* **35**, 1115 (2002).
- <sup>55</sup>J. Messud, P. M. Dinh, P.-G. Reinhard, and E. Suraud, “Improved Slater approximation to sic–oep,” *cpl* **461**, 316–320 (2008).
- <sup>56</sup>D. Pietezak and D. Vieira, “N-dependent self-interaction corrections: Are they still appealing?” *Theor. Chem. Acc.* **140**, 1–9 (2021).
- <sup>57</sup>J. Garza, J. A. Nichols, and D. A. Dixon, “The optimized effective potential and the self-interaction correction in density functional theory: Application to molecules,” *J. Chem. Phys.* **112**, 7880–7890 (2000), <https://doi.org/10.1063/1.481421>.
- <sup>58</sup>C. D. Pemmaraju, T. Archer, D. Sánchez-Portal, and S. Sanvito, “Atomic-orbital-based approximate self-interaction correction scheme for molecules and solids,” *Phys. Rev. B* **75**, 045101 (2007).
- <sup>59</sup>W. L. Luken and D. N. Beratan, “Localized orbitals and the Fermi hole,” *Theor. Chem. Acc.* **61**, 265–281 (1982).
- <sup>60</sup>W. L. Luken and J. C. Culbertson, “Localized orbitals based on the Fermi hole,” *Theor. Chem. Acc.* **66**, 279–293 (1984).
- <sup>61</sup>M. R. Pederson, A. Ruzsinszky, and J. P. Perdew, “Communication: Self-interaction correction with unitary invariance in density functional theory,” *J. Chem. Phys.* **140**, 121103 (2014), <https://doi.org/10.1063/1.4869581>.
- <sup>62</sup>M. R. Pederson and T. Baruah, “Chapter eight - self-interaction corrections within the Fermi-Orbital-based formalism,” in *Adv. At. Mol. Opt. Phys.*, Vol. 64, edited by E. Arimondo, C. C. Lin, and S. F. Yelin (Academic Press, 2015) pp. 153–180.
- <sup>63</sup>M. R. Pederson, “Fermi orbital derivatives in self-interaction corrected density functional theory: Applications to closed shell atoms,” *J. Chem. Phys.* **142**, 064112 (2015), <https://doi.org/10.1063/1.4907592>.
- <sup>64</sup>Z.-h. Yang, M. R. Pederson, and J. P. Perdew, “Full self-consistency in the Fermi-orbital self-interaction correction,” *Phys. Rev. A* **95**, 052505 (2017).
- <sup>65</sup>C. M. Diaz, T. Baruah, and R. R. Zope, “Fermi–Löwdin-orbital self-interaction correction using the optimized-effective-potential method within the Krieger-Li-Iafrate approximation,” *Phys. Rev. A* **103**, 042811 (2021).
- <sup>66</sup>C. M. Diaz, P. Suryanarayana, Q. Xu, T. Baruah, J. E. Pask, and R. R. Zope, “Implementation of Perdew–Zunger self-interaction correction in real space using Fermi–Löwdin orbitals,” *J. Chem. Phys.* **154**, 084112 (2021).
- <sup>67</sup>O. A. Vydrov, G. E. Scuseria, J. P. Perdew, A. Ruzsinszky, and G. I. Csonka, “Scaling down the Perdew–Zunger self-interaction correction in many-electron regions,” *J. Chem. Phys.* **124**, 094108 (2006).
- <sup>68</sup>J. P. Perdew, A. Ruzsinszky, J. Sun, and M. R. Pederson, “Chapter one - paradox of self-interaction correction: How can anything so right be so wrong?” in *Adv. At. Mol. Opt. Phys.*, Vol. 64 (Academic Press, 2015) pp. 1–14.
- <sup>69</sup>G. I. Csonka and B. G. Johnson, “Inclusion of exact exchange for self-interaction corrected h3 density functional potential energy surface,” *Theor. Chem. Acc.* **99**, 158–165 (1998).
- <sup>70</sup>A. I. Johnson, K. P. K. Withanage, K. Sharkas, Y. Yamamoto, T. Baruah, R. R. Zope, J. E. Peralta, and K. A. Jackson, “The effect of self-interaction error on electrostatic dipoles calculated using density functional theory,” *J. Chem. Phys.* **151**, 174106 (2019), <https://doi.org/10.1063/1.5125205>.
- <sup>71</sup>C. M. Diaz, L. Basurto, S. Adhikari, Y. Yamamoto, A. Ruzsinszky, T. Baruah, and R. R. Zope, “Self-interaction-corrected Kohn–Sham effective potentials using the density-consistent effective potential method,” *J. Chem. Phys.* **155**, 064109 (2021), <https://doi.org/10.1063/5.0056561>.
- <sup>72</sup>P. Bhattarai, B. Santra, K. Wagle, Y. Yamamoto, R. R. Zope, A. Ruzsinszky, K. A. Jackson, and J. P. Perdew, “Exploring and enhancing the accuracy of interior-scaled Perdew–Zunger self-interaction correction,” *J. Chem. Phys.* **154**, 094105 (2021).

- <sup>73</sup>S. Schwalbe, L. Fiedler, J. Kraus, J. Kortus, K. Trepte, and S. Lehtola, "PyFLOSIC: Python-based Fermi–Löwdin orbital self-interaction correction," *J. Chem. Phys.* **153**, 084104 (2020).
- <sup>74</sup>Y. Yamamoto, A. Salcedo, C. M. Diaz, M. S. Alam, T. Baruah, and R. R. Zope, "Assessing the effect of regularization on the molecular properties predicted by SCAN and self-interaction corrected SCAN meta-GGA," *Phys. Chem. Chem. Phys.* **22**, 18060–18070 (2020).
- <sup>75</sup>Y. Yamamoto, S. Romero, T. Baruah, and R. R. Zope, "Improvements in the orbitalwise scaling down of Perdew–Zunger self-interaction correction in many-electron regions," *J. Chem. Phys.* **152**, 174112 (2020).
- <sup>76</sup>S. Akter, Y. Yamamoto, R. R. Zope, and T. Baruah, "Static dipole polarizabilities of polyacenes using self-interaction-corrected density functional approximations," *J. Chem. Phys.* **154**, 114305 (2021), <https://doi.org/10.1063/5.0041265>.
- <sup>77</sup>S. Akter, J. A. Vargas, K. Sharkas, J. E. Peralta, K. A. Jackson, T. Baruah, and R. R. Zope, "How well do self-interaction corrections repair the overestimation of static polarizabilities in density functional calculations?" *Phys. Chem. Chem. Phys.* **23**, 18678–18685 (2021).
- <sup>78</sup>K. P. K. Withanage, S. Akter, C. Shahi, R. P. Joshi, C. Diaz, Y. Yamamoto, R. R. Zope, T. Baruah, J. P. Perdew, J. E. Peralta, and K. A. Jackson, "Self-interaction-free electric dipole polarizabilities for atoms and their ions using the Fermi–Löwdin self-interaction correction," *Phys. Rev. A* **100**, 012505 (2019).
- <sup>79</sup>S. Akter, Y. Yamamoto, C. M. Diaz, K. A. Jackson, R. R. Zope, and T. Baruah, "Study of self-interaction errors in density functional predictions of dipole polarizabilities and ionization energies of water clusters using Perdew–Zunger and locally scaled self-interaction corrected methods," *J. Chem. Phys.* **153**, 164304 (2020), <https://doi.org/10.1063/5.0025601>.
- <sup>80</sup>R. P. Joshi, K. Trepte, K. P. Withanage, K. Sharkas, Y. Yamamoto, L. Basurto, R. R. Zope, T. Baruah, K. A. Jackson, and J. E. Peralta, "Fermi–Löwdin orbital self-interaction correction to magnetic exchange couplings," *J. Chem. Phys.* **149**, 164101 (2018).
- <sup>81</sup>P. Mishra, Y. Yamamoto, P.-H. Chang, D. B. Nguyen, J. E. Peralta, T. Baruah, and R. R. Zope, "Study of self-interaction errors in density functional calculations of magnetic exchange coupling constants using three self-interaction correction methods," *J. Phys. Chem. A* **126**, 1923–1935 (2022), pMID: 35302373, <https://doi.org/10.1021/acs.jpca.1c10354>.
- <sup>82</sup>P. Mishra, Y. Yamamoto, J. K. Johnson, K. A. Jackson, R. R. Zope, and T. Baruah, "Study of self-interaction-errors in barrier heights using locally scaled and Perdew–Zunger self-interaction methods," *J. Chem. Phys.* **156**, 014306 (2022), <https://doi.org/10.1063/5.0070893>.
- <sup>83</sup>S. Romero, T. Baruah, and R. R. Zope, "Spin-state gaps and self-interaction-corrected density functional approximations: Octahedral Fe(II) complexes as case study," *J. Chem. Phys.* **158** (2023), 10.1063/5.0133999, 054305, [https://pubs.aip.org/aip/jcp/article-pdf/doi/10.1063/5.0133999/16704373/054305\\_1\\_online.pdf](https://pubs.aip.org/aip/jcp/article-pdf/doi/10.1063/5.0133999/16704373/054305_1_online.pdf).
- <sup>84</sup>L. Li, K. Trepte, K. A. Jackson, and J. K. Johnson, "Application of self-interaction corrected density functional theory to early, middle, and late transition states," *J. Phys. Chem. A* **124**, 8223–8234 (2020), pMID: 32883077.
- <sup>85</sup>A. Karanovich, Y. Yamamoto, K. A. Jackson, and K. Park, "Electronic structure of mononuclear Cu-based molecule from density-functional theory with self-interaction correction," *J. Chem. Phys.* **155**, 014106 (2021).
- <sup>86</sup>S. Schwalbe, T. Hahn, S. Liebing, K. Trepte, and J. Kortus, "Fermi–Löwdin orbital self-interaction corrected density functional theory: Ionization potentials and enthalpies of formation," *J. Comput. Chem.* **39**, 2463–2471 (2018), <https://onlinelibrary.wiley.com/doi/pdf/10.1002/jcc.25586>.
- <sup>87</sup>F. W. Aquino, R. Shinde, and B. M. Wong, "Fractional occupation numbers and self-interaction correction-scaling methods with the Fermi–Löwdin orbital self-interaction correction approach," *J. Comput. Chem.* **41**, 1200–1208 (2020), <https://onlinelibrary.wiley.com/doi/pdf/10.1002/jcc.26168>.
- <sup>88</sup>Y. Yamamoto, C. M. Diaz, L. Basurto, K. A. Jackson, T. Baruah, and R. R. Zope, "Fermi–Löwdin orbital self-interaction correction using the strongly constrained and appropriately normed meta-GGA functional," *J. Chem. Phys.* **151**, 154105 (2019), <https://doi.org/10.1063/1.5120532>.
- <sup>89</sup>K. P. K. Withanage, K. Trepte, J. E. Peralta, T. Baruah, R. Zope, and K. A. Jackson, "On the question of the total energy in the Fermi–Löwdin orbital self-interaction correction method," *J. Chem. Theory Comput.* **14**, 4122–4128 (2018), pMID: 29986131, <https://doi.org/10.1021/acs.jctc.8b00344>.
- <sup>90</sup>D.-y. Kao, K. Withanage, T. Hahn, J. Batool, J. Kortus, and K. Jackson, "Self-consistent self-interaction corrected density functional theory calculations for atoms using Fermi–Löwdin orbitals: Optimized fermi-orbital descriptors for Li–Kr," *J. Chem. Phys.* **147**, 164107 (2017), <https://doi.org/10.1063/1.4996498>.
- <sup>91</sup>K. P. K. Withanage, P. Bhattarai, J. E. Peralta, R. R. Zope, T. Baruah, J. P. Perdew, and K. A. Jackson, "Density-related properties from self-interaction corrected density functional theory calculations," *J. Chem. Phys.* **154**, 024102 (2021).
- <sup>92</sup>C. M. Diaz, L. Basurto, S. Adhikari, Y. Yamamoto, A. Ruzsinszky, T. Baruah, and R. R. Zope, "Self-interaction-corrected Kohn–Sham effective potentials using the density-consistent effective potential method," *J. Chem. Phys.* **155**, 064109 (2021).
- <sup>93</sup>D. B. Nguyen, M. R. Pederson, J. P. Perdew, K. A. Jackson, and J. E. Peralta, "Initial Fermi orbital descriptors for FLOSIC calculations: The quick-FOD method," *Chem. Phys. Lett.* **780**, 138952 (2021).
- <sup>94</sup>S. Schwalbe, K. Trepte, L. Fiedler, A. I. Johnson, J. Kraus, T. Hahn, J. E. Peralta, K. A. Jackson, and J. Kortus, "Interpretation and automatic generation of Fermi-orbital descriptors," *J. Comput. Chem.* **40**, 2843–2857 (2019).
- <sup>95</sup>K. Trepte, S. Schwalbe, S. Liebing, W. T. Schulze, J. Kortus, H. Myneni, A. V. Ivanov, and S. Lehtola, "Chemical bonding theories as guides for self-interaction corrected solutions: Multiple local minima and symmetry breaking," *J. Chem. Phys.* **155**, 224109 (2021).
- <sup>96</sup>K. Wagle, B. Santra, P. Bhattarai, C. Shahi, M. R. Pederson, K. A. Jackson, and J. P. Perdew, "Self-interaction correction in water-ion clusters," *J. Chem. Phys.* **154**, 094302 (2021).
- <sup>97</sup>K. Sharkas, K. Wagle, B. Santra, S. Akter, R. R. Zope, T. Baruah, K. A. Jackson, J. P. Perdew, and J. E. Peralta, "Self-interaction error overbinds water clusters but cancels in structural energy differences," *Proc. Natl. Acad. Sci.* **117**, 11283–11288 (2020), <https://www.pnas.org/content/117/21/11283.full.pdf>.
- <sup>98</sup>J. Vargas, P. Ufondu, T. Baruah, Y. Yamamoto, K. A. Jackson, and R. R. Zope, "Importance of self-interaction-error removal in density functional calculations on water cluster anions," *Phys. Chem. Chem. Phys.* **22**, 3789–3799 (2020).
- <sup>99</sup>K. Sharkas, L. Li, K. Trepte, K. P. K. Withanage, R. P. Joshi, R. R. Zope, T. Baruah, J. K. Johnson, K. A. Jackson, and J. E. Peralta, "Shrinking self-interaction errors with the Fermi–Löwdin orbital self-interaction-corrected density functional approximation," *J. Phys. Chem. A* **122**, 9307–9315 (2018).
- <sup>100</sup>K. Trepte, S. Schwalbe, T. Hahn, J. Kortus, D.-Y. Kao, Y. Yamamoto, T. Baruah, R. R. Zope, K. P. K. Withanage, J. E. Peralta, and K. A. Jackson, "Analytic atomic gradients in the Fermi–Löwdin orbital self-interaction correction," *J. Comput. Chem.* **40**, 820–825 (2019), <https://onlinelibrary.wiley.com/doi/pdf/10.1002/jcc.25767>.
- <sup>101</sup>B. Santra and J. P. Perdew, "Perdew–Zunger self-interaction correction: How wrong for uniform densities and large-Z atoms?" *J. Chem. Phys.* **150**, 174106 (2019), <https://doi.org/10.1063/1.5090534>.
- <sup>102</sup>C. Shahi, P. Bhattarai, K. Wagle, B. Santra, S. Schwalbe, T. Hahn, J. Kortus, K. A. Jackson, J. E. Peralta, K. Trepte, S. Lehtola, N. K. Nepal, H. Myneni, B. Neupane, S. Adhikari, A. Ruzsinszky, Y. Yamamoto, T. Baruah, R. R. Zope, and J. P. Perdew, "Stretched or noded orbital densities and self-interaction correction in density functional theory," *J. Chem. Phys.* **150**, 174102 (2019), <https://doi.org/10.1063/1.5087065>.

- <sup>103</sup>S. Ruan, K. A. Jackson, and A. Ruzsinszky, "Spin-crossover complexes: Self-interaction correction vs density correction," *The Journal of Chemical Physics* **158** (2023).
- <sup>104</sup>D. C. Liu and J. Nocedal, "On the limited memory BFGS method for large scale optimization," *Math. Program.* **45**, 503–528 (1989).
- <sup>105</sup>J. P. Perdew, J. A. Chevary, S. H. Vosko, K. A. Jackson, M. R. Pederson, D. J. Singh, and C. Fiolhais, "Atoms, molecules, solids, and surfaces: Applications of the generalized gradient approximation for exchange and correlation," *Phys. Rev. B* **46**, 6671–6687 (1992).
- <sup>106</sup>J. P. Perdew, K. Burke, and M. Ernzerhof, "Generalized gradient approximation made simple," *Phys. Rev. Lett.* **77**, 3865–3868 (1996).
- <sup>107</sup>J. P. Perdew, K. Burke, and M. Ernzerhof, "Generalized gradient approximation made simple [Phys. Rev. Lett. 77, 3865 (1996)]," *Phys. Rev. Lett.* **78**, 1396–1396 (1997).
- <sup>108</sup>J. W. Furness, A. D. Kaplan, J. Ning, J. P. Perdew, and J. Sun, "Accurate and numerically efficient  $r^2$ SCAN meta-generalized gradient approximation," *J. Phys. Chem. Lett.* **11**, 8208–8215 (2020), PMID: 32876454, <https://doi.org/10.1021/acs.jpclett.0c02405>.
- <sup>109</sup>R. R. Zope, T. Baruah, and K. A. Jackson, "FLOSIC 0.2," Based on the NRLMOL code of M. R. Pederson.
- <sup>110</sup>D. Porezag and M. R. Pederson, "Optimization of Gaussian basis sets for density-functional calculations," *Phys. Rev. A* **60**, 2840–2847 (1999).
- <sup>111</sup>J. M. Herbert and M. Head-Gordon, "Calculation of electron detachment energies for water cluster anions: An appraisal of electronic structure methods, with application to  $(\text{H}_2\text{O})_{20}^-$  and  $(\text{H}_2\text{O})_{24}^-$ ," *J. Phys. Chem. A* **109**, 5217–5229 (2005).
- <sup>112</sup>K. Yagi, Y. Okano, T. Sato, Y. Kawashima, T. Tsuneda, and K. Hirao, "Water cluster anions studied by the long-range corrected density functional theory," *J. Phys. Chem. A* **112**, 9845–9853 (2008), PMID: 18778041, <https://doi.org/10.1021/jp802927d>.
- <sup>113</sup>J. Doumont, F. Tran, and P. Blaha, "Implementation of self-consistent MGGA functionals in augmented plane wave based methods," *Phys. Rev. B* **105**, 195138 (2022).
- <sup>114</sup>A. P. Bartók and J. R. Yates, "Regularized SCAN functional," *J. Chem. Phys.* **150**, 161101 (2019), <https://doi.org/10.1063/1.5094646>.
- <sup>115</sup>D. Mejía-Rodríguez and S. B. Trickey, "Comment on "Regularized SCAN functional" [J. Chem. Phys. 150, 161101 (2019)]," *J. Chem. Phys.* **151**, 207101 (2019), <https://doi.org/10.1063/1.5120408>.
- <sup>116</sup>A. P. Bartók and J. R. Yates, "Response to "Comment on 'Regularized SCAN functional'" [J. Chem. Phys. 151, 207101 (2019)]," *J. Chem. Phys.* **151**, 207102 (2019), <https://doi.org/10.1063/1.5128484>.
- <sup>117</sup>P. J. Hay and W. R. Wadt, "Ab initio effective core potentials for molecular calculations. Potentials for K to Au including the outermost core orbitals," *J. Chem. Phys.* **82**, 299–310 (1985).
- <sup>118</sup>B. J. Lynch and D. G. Truhlar, "Small representative benchmarks for thermochemical calculations," *J. Phys. Chem. A* **107**, 8996–8999 (2003), <https://doi.org/10.1021/jp035287b>.
- <sup>119</sup>R. Peverati and D. G. Truhlar, "Communication: A global hybrid generalized gradient approximation to the exchange-correlation functional that satisfies the second-order density-gradient constraint and has broad applicability in chemistry," *J. Chem. Phys.* **135**, 191102 (2011), <https://doi.org/10.1063/1.3663871>.
- <sup>120</sup>R. R. Zope, Y. Yamamoto, C. M. Diaz, T. Baruah, J. E. Peralta, K. A. Jackson, B. Santra, and J. P. Perdew, "A step in the direction of resolving the paradox of Perdew-Zunger self-interaction correction," *J. Chem. Phys.* **151**, 214108 (2019).
- <sup>121</sup>P. Mishra, Y. Yamamoto, J. K. Johnson, K. A. Jackson, R. R. Zope, and T. Baruah, "Study of self-interaction-errors in barrier heights using locally scaled and Perdew–Zunger self-interaction methods," *J. Chem. Phys.* **156**, 014306 (2022).
- <sup>122</sup>A. Karton, R. J. O'Reilly, and L. Radom, "Assessment of theoretical procedures for calculating barrier heights for a diverse set of water-catalyzed proton-transfer reactions," *J. Phys. Chem. A* **116**, 4211–4221 (2012).
- <sup>123</sup>J. F. Janak, "Proof that  $\frac{\partial \epsilon}{\partial n_i} = \epsilon$  in density-functional theory," *Phys. Rev. B* **18**, 7165–7168 (1978).
- <sup>124</sup>M. Levy, J. P. Perdew, and V. Sahni, "Exact differential equation for the density and ionization energy of a many-particle system," *Phys. Rev. A* **30**, 2745–2748 (1984).
- <sup>125</sup>M. K. Harbola, "Relationship between the highest occupied Kohn-Sham orbital eigenvalue and ionization energy," *Phys. Rev. B* **60**, 4545–4550 (1999).
- <sup>126</sup>J. P. Perdew and M. Levy, "Comment on "Significance of the highest occupied Kohn-Sham eigenvalue","" *Phys. Rev. B* **56**, 16021 (1997).
- <sup>127</sup>E. Alizadeh and L. Sanche, "Precursors of solvated electrons in radiobiological physics and chemistry," *Chem. Rev.* **112**, 5578–5602 (2012).
- <sup>128</sup>J. M. Herbert and M. P. Coons, "The hydrated electron," *Annu. Rev. Phys. Chem.* **68**, 447–472 (2017).
- <sup>129</sup>J. Miralles, J.-P. Daudey, and R. Caballol, "Variational calculation of small energy differences. The singlet-triplet gap in  $[\text{Cu}_2\text{Cl}_6]^{2-}$ ," *Chem. Phys. Lett.* **198**, 555–562 (1992).
- <sup>130</sup>O. Castell, J. Miralles, and R. Caballol, "Structural dependence of the singlet-triplet gap in doubly bridged copper dimers: A variational CI calculation," *Chem. Phys.* **179**, 377–384 (1994).
- <sup>131</sup>L. Noodleman, "Valence bond description of antiferromagnetic coupling in transition metal dimers," *J. Chem. Phys.* **74**, 5737–5743 (1981).
- <sup>132</sup>R. D. Willett, D. Gatteschi, and O. Kahn, "Magneto-structural correlations in exchange coupled systems," *Tech. Rep.* (D. Reidel Publishing Co., Hingham, MA, 1985).
- <sup>133</sup>K. Ray, T. Weyhermüller, F. Neese, and K. Wieghardt, "Electronic structure of square planar bis (benzene-1, 2-dithiolato) metal complexes  $[\text{M}(\text{I})_2]_z$  ( $z = 2-, 1-, 0$ ;  $m = \text{ni, pd, pt, cu, au}$ ): An experimental, density functional, and correlated ab initio study," *Inorg. Chem.* **44**, 5345–5360 (2005).
- <sup>134</sup>M. S. Fataftah, M. D. Krzyaniak, B. Vlasisavljevic, M. R. Wasielewski, J. M. Zadrozny, and D. E. Freedman, "Metal–ligand covalency enables room temperature molecular qubit candidates," *Chem. Sci.* **10**, 6707–6714 (2019).
- <sup>135</sup>B. K. Maiti, L. B. Maia, K. Pal, B. Pakhira, T. Avilés, I. Moura, S. R. Pauleta, J. L. Nuñez, A. C. Rizzi, C. D. Brondino, et al., "One electron reduced square planar bis (benzene-1, 2-dithiolato) copper dianionic complex and redox switch by  $\text{O}_2/\text{HO}^-$ ," *Inorg. Chem.* **53**, 12799–12808 (2014).